# Localization and limit laws of a three-state alternate quantum walk on a two-dimensional lattice

Takuya Machida[1] and C. M. Chandrashekar[2]

[1]*Japan Society for the Promotion of Science, Kojimachi Business Center Building, 5-3-1 Kojimachi, Chiyoda-ku, Tokyo 102-0083, Japan*

[2]*Optics and Quantum Information Group, The Institute of Mathematical Sciences, C.I.T. Campus, Taramani, Chennai 600113, India*

(Received 10 October 2015; published 3 December 2015)

A two-dimensional discrete-time quantum walk (DTQW) can be realized by alternating a two-state DTQW in one spatial dimension followed by an evolution in the other dimension. This was shown to reproduce a probability distribution for a certain configuration of a four-state DTQW on a two-dimensional lattice. In this work we present a three-state alternate DTQW with a parametrized coin-flip operator and show that it can produce localization that is also observed for a certain other configuration of the four-state DTQW and nonreproducible using the two-state alternate DTQW. We will present two limit theorems for the three-state alternate DTQW. One of the limit theorems describes a long-time limit of a return probability, and the other presents a convergence in distribution for the position of the walker on a rescaled space by time. We find that the spatial entanglement generated by the three-state alternate DTQW is higher than that by the four-state DTQW. Using all our results, we outline the relevance of these walks in three-level physical systems.

DOI: 10.1103/PhysRevA.92.062307 PACS number(s): 03.67.Lx, 02.50.Cw

## I. INTRODUCTION

Quantum walks have played an important role in the area of quantum information and computation. Particularly, quantum walks have been effectively used to propose quantum algorithms [1] and as a tool to realize universal quantum computation [2,3]. They still continue to garner interest in simulating quantum dynamics in various physical systems and manifest the interesting phenomenon observed in real systems such as photosynthesis [4] and edge states [5]. Therefore, detailed studies of quantum walks and their long-time behavior in various configurations will give a better understanding of controllable evolutions, paving the way for further simulating the quantum dynamics in various physically relevant systems and for engineering the quantum dynamics for the required specifications. Experimental implementation of quantum walks in various physical systems, for example, single atom in an optical lattice [6], two-photon optical fiber networks [7], and interacting bosonic atoms in an optical lattice [8], have demonstrated the accessibility of systems via quantum walks.

A discrete-time quantum walk (DTQW) on a one-dimensional position space is defined using a two-state system which is referred to as a coin state. Its evolution is described using a quantum coin operation acting on a coin space followed by a position-shift operator to evolve the system coherently in superposition among different locations on a position space. The extension of the DTQW to a higher spatial dimension was successfully demonstrated by expanding the dimension of the coin space [9]. For a two-dimensional DTQW with a four-state coin space, a long-time limit distribution (theorem) was obtained by Watabe *et al.* [10]. The limit theorem for the four-state DTQW was determined by a parametrized coin-flip operator which contained a Grover coin, and its limit density function was shown to feature a Dirac $\delta$ function highlighting a localized component and a continuous function with a compact support representing a diffusing component. The clear spread of probability distribution of the four-state DTQW with time indicating the absence of the Dirac $\delta$ function was realized only for a particular composition of the initial state of the walk and the coin-flip operation.

However, an extended coin space with control over the internal states to implement the corresponding coin operations is an extremely challenging task for physical implementation of the DTQW in higher dimensions. Therefore, an alternate scheme to implement a DTQW on a two-dimensional position space using a two-state system was introduced [11,12]. The two-state DTQW was first evolved in one spatial dimension followed by an evolution in the other dimension, and this process of the alternate evolution was repeated to implement a large number of steps of the walk. This two-state alternate DTQW was shown to manifest the wide spread probability distribution for a specific configuration of a four-state DTQW on a two-dimensional position space. The long-time limit distribution describing the asymptotic behavior of the two-state alternate DTQW after a large number of steps has also been reported [13]. The absence of Dirac $\delta$ functions in the limit density function of the two-state alternate DTQW is helpful in understanding the similarities with the limit distribution function obtained for a particular configuration of the four-state DTQW. Various properties of the two-state alternate DTQW on an $N$-dimensional space was later reported [14,15]. The effect of noise on the two-state alternate DTQW and a four-state Grover walk was also studied and the robustness of the two-state walk over the four-state walk in the presence of noise was shown [16]. None of these studies on the two-state alternate walks reported the presence of a Dirac $\delta$ function in the limit distribution as it was reported for some configurations of the four-state DTQW. The absence of constant eigenvalues in the Fourier picture of the two-state alternate DTQW has been a reason for the nonlocalized evolutions. However, later the existence of a time-dependent two-state alternate DTQW with periodic coin operators, which are based on the products of a Hadamard operator and phase-shift operators depending on time, was shown to manifest localization [14]. This still leaves open the question of an alternate DTQW configuration which can manifest localization without any complex combination of coin operations.

The first theoretical study of a three-state Grover walk on a one-dimensional position space reported localization around an initial position [17]. Since then, the three-state DTQW on

 

the line with a parametrized coin operator and its dependency on the initial state were examined theoretically and numerically [18–21]. Motivated by the past studies, we extend them to a three-state alternate DTQW in two dimensions in this paper. We show that the three-state alternate DTQW localizes around the initial position. We make an approximate analysis for probability amplitudes of the three-state DTQW. Particularly, defining a return probability as just the probability of finding the walker at the origin, we compute its long-time limit from the approximate behavior of the walk. On the other hand, we also focus on a rescaled space and give a convergence law for the DTQW. The limit law shows a behavior of the walker on the rescaled space at an infinite time and the density function in that law consists of both a Dirac $\delta$ function which implies the possibility of localization and a continuous function with a compact support. We discuss localization from the point of view of both the return probability on the nonrescaled space and a convergence in distribution on the rescaled space.

In the Sec. II we introduce the three-state alternate DTQW on a two-dimensional square lattice, and two limit theorems are given with their proofs in subsequent sections. One is a long-time limit of the return probability (Sec. III) and the other is a long-time convergence in distribution on the rescaled space (Sec. IV). In Sec. V we present an entanglement generated between the coin and position space, and between the two spatial dimensions for both forms, the three-state and the four-state DTQW. We compare the observations and briefly discuss the possibility of physical realization of the three-state DTQW in a three-level atomic system. In Sec. VI, we summarize our results and discuss future prospects.

## II. DEFINITION OF A THREE-STATE ALTERNATE QUANTUM WALK ON A SQUARE LATTICE

In this section, we define a three-state alternate DTQW on a two-dimensional square lattice. The position of the walker is expressed on two Hilbert spaces $\mathcal{H}_p$ and $\mathcal{H}_c$. The Hilbert space $\mathcal{H}_c$ is spanned by an orthogonal normal basis $\{|x,y\rangle : x,y \in \mathbb{Z}\}$, where $\mathbb{Z} = \{0,\pm1,\pm2,\ldots\}$. Since the Hilbert space represents the space in which the walker locates, it is called the position Hilbert space. At each vertex on the position Hilbert space $\mathcal{H}_p$, the walker can be expressed in superposition of three coin states. Therefore, the coin Hilbert space $\mathcal{H}_c$ is spanned by an orthogonal normal basis $\{|0\rangle, |1\rangle, |2\rangle\}$. To compute limit laws later, we take the following orthonormal vectors:

$$|0\rangle = \begin{bmatrix}1\\0\\0\end{bmatrix}, \quad |1\rangle = \begin{bmatrix}0\\1\\0\end{bmatrix}, \quad |2\rangle = \begin{bmatrix}0\\0\\1\end{bmatrix}. \tag{1}$$

The whole state $|\Psi_t\rangle$ of the quantum walker at time $t \in \{0,1,2,\ldots\}$ is described on the tensor Hilbert space $\mathcal{H}_p \otimes \mathcal{H}_c$. The position of the walker is shifted by two position-shift operators $S_1$ and $S_2$ after the superposition is operated by a coin-flip operator $C$ as follows:

$$|\Psi_{t+1}\rangle = S_2 C S_1 C |\Psi_t\rangle, \tag{2}$$

where

$$S_1 = \sum_{x,y\in\mathbb{Z}} |x-1,y\rangle\langle x,y| \otimes |0\rangle\langle 0| + |x,y\rangle\langle x,y| \otimes |1\rangle\langle 1| + |x+1,y\rangle\langle x,y| \otimes |2\rangle\langle 2|, \tag{3}$$

$$S_2 = \sum_{x,y\in\mathbb{Z}} |x,y-1\rangle\langle x,y| \otimes |0\rangle\langle 0| + |x,y\rangle\langle x,y| \otimes |1\rangle\langle 1| + |x,y+1\rangle\langle x,y| \otimes |2\rangle\langle 2|, \tag{4}$$

and

$$\begin{aligned} C &= \sum_{x,y\in\mathbb{Z}} |x,y\rangle\langle x,y| \otimes \left(-\frac{1+c}{2}|0\rangle\langle 0| + \frac{s}{\sqrt{2}}|0\rangle\langle 1| + \frac{1-c}{2}|0\rangle\langle 2| + \frac{s}{\sqrt{2}}|1\rangle\langle 0| + c|1\rangle\langle 1|\right.\\ &\quad \left. + \frac{s}{\sqrt{2}}|1\rangle\langle 2| + \frac{1-c}{2}|2\rangle\langle 0| + \frac{s}{\sqrt{2}}|2\rangle\langle 1| - \frac{1+c}{\sqrt{2}}|2\rangle\langle 2|\right)\\ &= \sum_{x,y\in\mathbb{Z}} |x,y\rangle\langle x,y| \otimes \begin{bmatrix} -\frac{1+c}{2} & \frac{s}{\sqrt{2}} & \frac{1-c}{2}\\ \frac{s}{\sqrt{2}} & c & \frac{s}{\sqrt{2}}\\ \frac{1-c}{2} & \frac{s}{\sqrt{2}} & -\frac{1+c}{2}\end{bmatrix}, \end{aligned} \tag{5}$$

with $c = \cos\theta$ and $s = \sin\theta$ [$\theta \in [0,2\pi)$]. Since the behavior of the walker is obvious at $\theta = 0,\pi$, we will not treat them. The position-shift operator $S_1$ ($S_2$) plays a role of moving the walker to the $x$ ($y$) direction, as shown in Fig. 1.

When we set $c = -1/3$ and $s = 2\sqrt{2}/3$, the coin-flip operator $C$ becomes a Grover coin

$$C = \sum_{x,y\in\mathbb{Z}} |x,y\rangle\langle x,y| \otimes \begin{bmatrix} -\frac{1}{3} & \frac{2}{3} & \frac{2}{3}\\ \frac{2}{3} & -\frac{1}{3} & \frac{2}{3}\\ \frac{2}{3} & \frac{2}{3} & -\frac{1}{3}\end{bmatrix}. \tag{6}$$

The probability that the walker is observed at position $(x,y) \in \mathbb{Z}$ is defined by

$$\mathbb{P}[(X_t,Y_t) = (x,y)] = \langle\Psi_t| \left(|x,y\rangle\langle x,y| \otimes \sum_{j=0}^{2} |j\rangle\langle j|\right) |\Psi_t\rangle, \tag{7}$$

where $(X_t,Y_t) \in \mathbb{Z}^2$ denotes the position of the walker at time $t$. Finally we set an initial condition

$$|\Psi_0\rangle = |0,0\rangle \otimes (\alpha|0\rangle + \beta|1\rangle + \gamma|2\rangle), \tag{8}$$

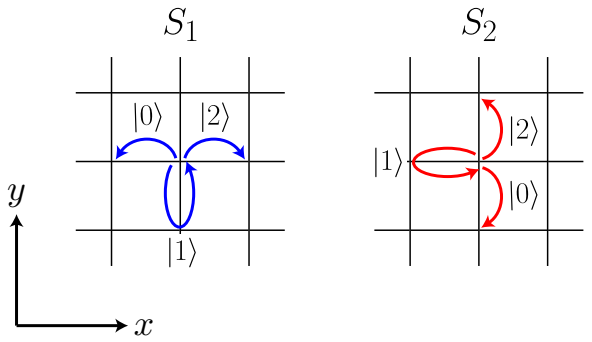


FIG. 1. (Color online) The position-shift operator $S_1$ ($S_2$) shifts the walker to the $x$ ($y$) direction.

for $\alpha,\beta$, and $\gamma \in \mathbb{C}$ such that $|\alpha|^2+|\beta|^2+|\gamma|^2=1$, where $\mathbb{C}$ means the set of complex numbers. Figure 2 illustrates two examples of the probability distribution in Eq. (7) and we observe localization around the origin in the pictures.

## III. LIMIT LAW OF A RETURN PROBABILITY

The study of return probabilities is a topic of research interest in the field of random walks as well as quantum walks. Although there is an analytical result for a return probability of a one-dimensional DTQW as $t \to \infty$ [22], we have not had any rigorous result for two-dimensional walks. Ide *et al.* [22] computed a limit value of the return probability when the walker starts from a certain position, and simultaneously proved localization of the walk. In this section we concentrate on a return probability of the three-state alternate walk. Since the walker starts from the origin, we consider the return probability as the probability that the walker can be observed at the origin. That is, the return probability at time $t$ is determined by the probability $\mathbb{P}[(X_t,Y_t)=(0,0)]$. As $t\to\infty$, we obtain the following limit theorem about the return probability.

*Theorem 1.* The return probability is of the form

$$\lim_{t\to\infty}\mathbb{P}[(X_t,Y_t)=(0,0)]=\begin{cases}|\eta_1(\theta;\alpha,\beta,\gamma)|^2+|\eta_2(\theta;\alpha,\beta,\gamma)|^2+|\eta_1(\theta;\gamma,\beta,\alpha)|^2 & (0<\theta<\pi),\\ |\eta_1(\theta-\pi;\alpha,\beta,\gamma)|^2+|\eta_2(\theta-\pi;\alpha,\beta,\gamma)|^2+|\eta_1(\theta-\pi;\gamma,\beta,\alpha)|^2 & (\pi<\theta<2\pi),\end{cases} \tag{9}$$

where

$$\eta_1(\theta;\alpha,\beta,\gamma)=g_3(\theta)\alpha+\tfrac{1}{2}g_2(\theta)\beta+\tfrac{1}{2}g_1(\theta)\gamma, \tag{10}$$

$$\eta_2(\theta;\alpha,\beta,\gamma)=\tfrac{1}{2}g_2(\theta)(\alpha+\gamma)+[1-2g_3(\theta)]\beta, \tag{11}$$

and

$$g_1(\theta)=\frac{2\{\pi(1-c)^2-s(3+c^2)+4c\theta\}}{\pi s}, \tag{12}$$

$$g_2(\theta)=\frac{\sqrt{2}\{\pi(1-c)+2(cs-\theta)\}}{\pi s}, \tag{13}$$

$$g_3(\theta)=\frac{s}{\pi}. \tag{14}$$

*Proof.* We use a method based on the Fourier analysis to compute the limit of the return probability. The Fourier analysis was introduced to quantum walks by Grimmett *et al.* [23]. First, we define the Fourier transform $|\hat{\Psi}_t(a,b)\rangle \in \mathbb{C}^3$ $[a,b\in[-\pi,\pi)]$ of the walk at time $t$ as

$$|\hat{\Psi}_t(a,b)\rangle=\sum_{x,y\in\mathbb{Z}}e^{-i(ax+by)}|\psi_t(x,y)\rangle\,. \tag{15}$$

The amplitude at position $(x,y)\in\mathbb{Z}^2$ is extracted by using the inverse Fourier transform

$$|\psi_t(x,y)\rangle=\int_{-\pi}^{\pi}\frac{da}{2\pi}\int_{-\pi}^{\pi}\frac{db}{2\pi}\,e^{i(ax+by)}|\hat{\Psi}_t(a,b)\rangle\,, \tag{16}$$

Equation (2) leads us to the time evolution of the Fourier transform

$$|\hat{\Psi}_t(a,b)\rangle=R(b)\hat{C}R(a)\hat{C}\,|\hat{\Psi}_t(a,b)\rangle\,, \tag{17}$$

where

$$\hat{C}=\begin{bmatrix}-\frac{1+c}{2} & \frac{s}{\sqrt{2}} & \frac{1-c}{2}\\ \frac{s}{\sqrt{2}} & c & \frac{s}{\sqrt{2}}\\ \frac{1-c}{2} & \frac{s}{\sqrt{2}} & -\frac{1+c}{2}\end{bmatrix},\quad R(k)=\begin{bmatrix}e^{ik}&0&0\\0&1&0\\0&0&e^{-ik}\end{bmatrix}. \tag{18}$$

From Eq. (17), the Fourier transform at time $t$ becomes $|\hat{\Psi}_t(a,b)\rangle=[R(b)\hat{C}R(a)\hat{C}]^t\,|\hat{\Psi}_0(a,b)\rangle$. We express the eigenvalues $\lambda_j(a,b)$ $(j=1,2,3)$ of the unitary matrix $R(b)\hat{C}R(a)\hat{C}$ as follows:

$$\lambda_j(a,b)=e^{i\nu_j(a,b)}\quad(j=1,2,3), \tag{19}$$

with

$$\nu_1(a,b)=0, \tag{20}$$

$$\nu_2(a,b)=2\arccos\left[\frac{1+c}{2}\cos\left(\frac{a+b}{2}\right)+\frac{1-c}{2}\cos\left(\frac{a-b}{2}\right)\right], \tag{21}$$

$$\nu_3(a,b)=-2\arccos\left[\frac{1+c}{2}\cos\left(\frac{a+b}{2}\right)+\frac{1-c}{2}\cos\left(\frac{a-b}{2}\right)\right]. \tag{22}$$

The components of the normalized eigenvector $|v_j(a,b)\rangle$ $(j=1,2,3)$ associated with the eigenvalue $\lambda_j(a,b)$ are given by

$$\langle 0|v_j(a,b)\rangle=-\frac{s(1-e^{-ia})}{\sqrt{N_j(a,b)}}[e^{ib}\{(1+c)e^{ia}+1-c\}\lambda_j(a,b)-\{(1-c)e^{ia}+1+c\}], \tag{23}$$

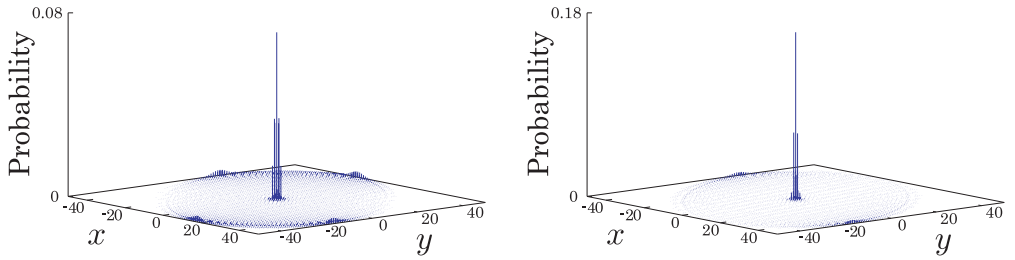


(a) $\alpha = \beta = \gamma = 1/\sqrt{3}$ (b) $\alpha = \gamma = 0,\ \beta = 1$

FIG. 2. (Color online) Probability distribution of three-state alternate quantum walk at time $t = 50$ on a two-dimensional lattice using the coin-flip operator with parameters $c = -1/3$, $s = 2\sqrt{2}/3$. Localization of the probability distribution indicating an alternate walk with two different initial states is shown in (a) and (b).

$$\langle 1|v_j(a,b)\rangle = \frac{2\sqrt{2}}{\sqrt{N_j(a,b)}}[\lambda_j(a,b)^2 - \{(1+c^2)\cos a\cos b - 2c\sin a\sin b + s^2\cos b\}\lambda_j(a,b) + s^2\cos a + c^2], \tag{24}$$

$$\langle 2|v_j(a,b)\rangle = \frac{s(1-e^{-ia})}{\sqrt{N_j(a,b)}}[e^{-ib}\{(1-c)e^{ia} + 1 + c\}\lambda_j(a,b) - \{(1+c)e^{ia} + 1 - c\}], \tag{25}$$

where $N_j(a,b)\,(j = 1,2,3)$ is a normalized factor.

Here, we define a function

$$F(x,y) = \int_{-\pi}^{\pi}\frac{da}{2\pi}\int_{-\pi}^{\pi}\frac{db}{2\pi}\,\frac{e^{i(ax+by)}}{16\left\{1 - \left[\frac{1+c}{2}\cos\left(\frac{a+b}{2}\right) + \frac{1-c}{2}\cos\left(\frac{a-b}{2}\right)\right]^2\right\}} \quad (x,y \in \mathbb{Z}). \tag{26}$$

We use this function later to express the asymptotic behavior of the probability amplitude $|\psi_t(x,y)\rangle$ after many steps. By using the residue theorem in Eq. (26), we get an integral representation of the function $F(x,y)$

$$F(x,y) = \frac{1}{8\pi(1-c)}\int_0^{\frac{\pi}{2}}\cos[(x+y)k]\left\{\frac{[w_1(k) - \sqrt{w_1(k)^2-1}]^{|x-y|}}{\sqrt{w_1(k)^2-1}} + \frac{[w_2(k) + \sqrt{w_2(k)^2-1}]^{|x-y|}}{\sqrt{w_2(k)^2-1}}\right\}dk, \tag{27}$$

where

$$w_1(k) = \frac{2-(1+c)\cos k}{1-c}, \quad w_2(k) = \frac{-2-(1+c)\cos k}{1-c}. \tag{28}$$

Again, we get a long-time asymptotic behavior of the amplitude at position $(x,y) \in \mathbb{Z}^2$

$$\begin{aligned}|\psi_t(x,y)\rangle &= \int_{-\pi}^{\pi}\frac{da}{2\pi}\int_{-\pi}^{\pi}\frac{db}{2\pi}\sum_{j=1}^{3}e^{i(ax+by)}\lambda_j(a,b)^t\,\langle v_j(a,b)|\hat{\Psi}_0(a,b)\rangle\,|v_j(a,b)\rangle \\ &\sim \int_{-\pi}^{\pi}\frac{da}{2\pi}\int_{-\pi}^{\pi}\frac{db}{2\pi}\,e^{i(ax+by)}\,\langle v_1(a,b)|\hat{\Psi}_0(a,b)\rangle\,|v_1(a,b)\rangle \quad (t\to\infty),\end{aligned} \tag{29}$$

where $h_1(t) \sim h_2(t)\,(t\to\infty)$ means $\lim_{t\to\infty} h_1(t)/h_2(t) = 1$. The Riemann-Lebesgue lemma has been used in Eq. (29). We are also allowed to employ another form of the eigenvector

$$|v_1(k)\rangle = \frac{1}{\sqrt{\tilde{N}_1(k)}}\begin{bmatrix}\sqrt{2}s(e^{i(a+b)/2} - e^{-i(a-b)/2}) \\ 2i\{(1+c)\sin[(a+b)/2] - (1-c)\sin[(a-b)/2]\} \\ -\sqrt{2}s(e^{-i(a+b)/2} - e^{i(a-b)/2})\end{bmatrix}, \tag{30}$$

with

$$\tilde{N}_1(a,b) = 16\left\{1 - \left[\frac{1+c}{2}\cos\left(\frac{a+b}{2}\right) + \frac{1-c}{2}\cos\left(\frac{a-b}{2}\right)\right]^2\right\}. \tag{31}$$

Estimating Eq. (29) with Eq. (30), we have an expression of the asymptotic behavior of the probability amplitude $|\psi_t(x,y)\rangle$ at a large enough time,

$$\begin{aligned}\langle 0|\psi_t(x,y)\rangle \sim{}& \sqrt{2}s\{-A(\alpha,\beta)F(x-1,y)-B(\gamma,\beta)F(x-1,y+1)+[A(\alpha,\beta)+B(\alpha,\beta)]F(x,y)\\ &+[A(\gamma,\beta)+B(\gamma,\beta)]F(x,y+1)-B(\alpha,\beta)F(x+1,y)-A(\gamma,\beta)F(x+1,y+1)\},\end{aligned} \tag{32}$$

$$\begin{aligned}\langle 1|\psi_t(x,y)\rangle \sim{}&(1+c)[-A(\alpha,\beta)F(x-1,y-1)-B(\gamma,\beta)F(x-1,y)+B(\alpha,\beta)F(x,y-1)+A(\alpha+\gamma,2\beta)F(x,y)\\ &+B(\gamma,\beta)F(x,y+1)-B(\alpha,\beta)F(x+1,y)-A(\gamma,\beta)F(x+1,y+1)]\\ &-(1-c)[-A(\alpha,\beta)F(x-1,y)-B(\gamma,\beta)F(x-1,y+1)+A(\alpha,\beta)F(x,y-1)+B(\alpha+\gamma,2\beta)F(x,y)\\ &+A(\gamma,\beta)F(x,y+1)-B(\alpha,\beta)F(x+1,y-1)-A(\gamma,\beta)F(x+1,y)],\end{aligned} \tag{33}$$

$$\begin{aligned}\langle 2|\psi_t(x,y)\rangle \sim{}&\sqrt{2}s\{-A(\alpha,\beta)F(x-1,y-1)-B(\gamma,\beta)F(x-1,y)+[A(\alpha,\beta)+B(\alpha,\beta)]F(x,y-1)\\ &+[A(\gamma,\beta)+B(\gamma,\beta)]F(x,y)-B(\alpha,\beta)F(x+1,y-1)-A(\gamma,\beta)F(x+1,y)\},\end{aligned} \tag{34}$$

where

$$A(z_1,z_2)=\sqrt{2}sz_1+(1+c)z_2,\quad B(z_1,z_2)=\sqrt{2}sz_1-(1-c)z_2. \tag{35}$$

Computing the long-time asymptotic behavior of the amplitude at the origin, we obtain

$$|\psi_t(0,0)\rangle \sim \begin{cases}\begin{bmatrix} g_3(\theta)\alpha+\frac{1}{2}g_2(\theta)\beta+\frac{1}{2}g_1(\theta)\gamma \\ \frac{1}{2}g_2(\theta)(\alpha+\gamma)+(1-2g_3(\theta))\beta \\ \frac{1}{2}g_1(\theta)\alpha+\frac{1}{2}g_2(\theta)\beta+g_3(\theta)\gamma, \end{bmatrix} & (0<\theta<\pi)\\ \begin{bmatrix} g_3(\theta-\pi)\alpha+\frac{1}{2}g_2(\theta-\pi)\beta+\frac{1}{2}g_1(\theta-\pi)\gamma \\ \frac{1}{2}g_2(\theta-\pi)(\alpha+\gamma)+(1-2g_3(\theta-\pi))\beta \\ \frac{1}{2}g_1(\theta-\pi)\alpha+\frac{1}{2}g_2(\theta-\pi)\beta+g_3(\theta-\pi)\gamma \end{bmatrix} & (\pi<\theta<2\pi),\end{cases} \tag{36}$$

recalling the functions $g_j(\theta)$ $(j=1,2,3)$ in Eqs. (12)–(14). The limit of the return probability follows from Eq. (36). ■

In Fig. 3 we show the return probability for two different initial states of the walk. We can see that the probability converges to the limit as time $t$ goes up. In Fig. 4 we show the probability at time 100 and at the limit with regard to the parameter $\theta$, which determines the coin-flip operator $C$.

## IV. CONVERGENCE IN DISTRIBUTION ON A RESCALED SPACE BY TIME

In the previous section, we concentrated on the probability $\mathbb{P}[(X_t,Y_t)=(x,y)]$ and computed the long-time limit of the return probability $\mathbb{P}[(X_t,Y_t)=(0,0)]$. In this section we will present a convergence theorem on a rescaled space by time. This theorem shows us the overall behavior of the walker after many steps.

*Theorem 2.* The three-state alternate DTQW starting from the origin has a convergence law

$$\begin{aligned}&\lim_{t\to\infty}\mathbb{P}\left(\frac{X_t}{t}\leqslant x,\frac{Y_t}{t}\leqslant y\right)\\ &\quad=\int_{-\infty}^{x}du\int_{-\infty}^{y}dv\left\{\Delta(\theta;\alpha,\beta,\gamma)\delta_o(u,v)\right.\\ &\qquad\left.+\frac{\xi(u,v;\alpha,\beta,\gamma)}{2\pi^2(1-u^2)(1-v^2)}I_{\mathcal{D}}(u,v)\right\},\end{aligned} \tag{37}$$

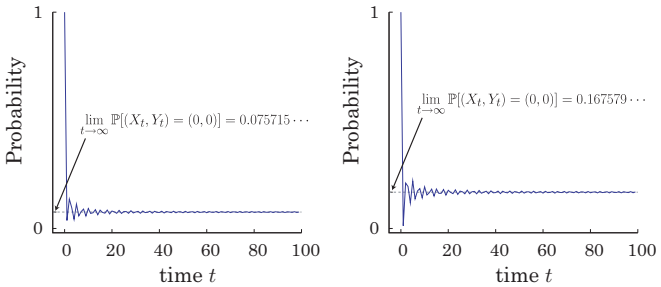


(a) $\alpha=\beta=\gamma=1/\sqrt{3}$ (b) $\alpha=\gamma=0$, $\beta=1$

FIG. 3. (Color online) Given the parameter $\theta$ which satisfies $\cos\theta=-1/3$ and $\sin\theta=2\sqrt{2}/3$, the left (right) figure shows how the return probability $\mathbb{P}[(X_t,Y_t)=(0,0)]$ depends on time $t$ in the case of $\alpha=\beta=\gamma=1/\sqrt{3}$ ($\alpha=\gamma=0$, $\beta=1$).

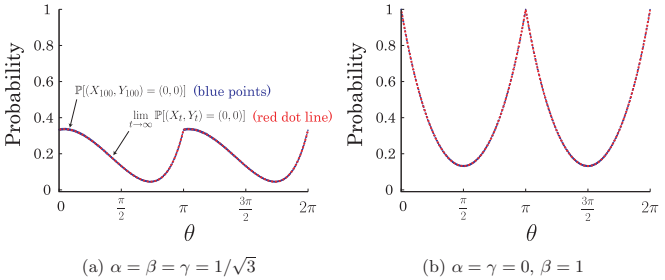


(a) $\alpha=\beta=\gamma=1/\sqrt{3}$ (b) $\alpha=\gamma=0$, $\beta=1$

FIG. 4. (Color online) Return probability at time 100 (blue points) and the limit (red dot line) for evolution with different initial states are shown in (a) and (b). We observe the clear overlap of the walk being found at the origin at time 100, and its limit as $t\to\infty$. The positive value of the limit implies localization of the walker at the origin.

where $\delta_o(x,y)$ denotes a Dirac $\delta$ function at the origin and

$$\Delta(\theta;\alpha,\beta,\gamma)=\begin{cases}|\beta|^2+\mathrm{Re}(\alpha\overline{\gamma})g_1(\theta)+\mathrm{Re}[(\alpha+\gamma)\overline{\beta}]g_2(\theta)+(1-3|\beta|^2)g_3(\theta) & (0<\theta<\pi),\\ |\beta|^2+\mathrm{Re}(\alpha\overline{\gamma})g_1(\theta-\pi)+\mathrm{Re}[(\alpha+\gamma)\overline{\beta}]g_2(\theta-\pi)+(1-3|\beta|^2)g_3(\theta-\pi) & (\pi<\theta<2\pi),\end{cases} \tag{38}$$

$$\xi(x,y;\alpha,\beta,\gamma)=(1-y)^2|\alpha|^2+2(1-y^2)|\beta|^2+(1+y)^2|\gamma|^2+\frac{2\sqrt{2}(x-cy)(1-y)}{s}\mathrm{Re}(\alpha\overline{\beta})$$
$$-\frac{2\sqrt{2}(x-cy)(1+y)}{s}\mathrm{Re}(\beta\overline{\gamma})+\frac{2\{s^2-2x^2-(1+c^2)y^2+4cxy\}}{s^2}\mathrm{Re}(\alpha\overline{\gamma}), \tag{39}$$

$$\mathcal{D}=\left\{(x,y)\in\mathbb{R}^2\,\middle|\,\frac{(x+y)^2}{2(1+c)}+\frac{(x-y)^2}{2(1-c)}<1\right\}. \tag{40}$$

*Proof.* Using the eigenvalues $\lambda_j(a,b)$ and the normalized eigenvectors $|v_j(a,b)\rangle$ $(j=1,2,3)$ of the matrix $R(b)\hat{C}R(a)\hat{C}$, the $(r_1,r_2)$th joint moments $(r_1,r_2=0,1,2,\ldots)$ of the random variable $(X_t,Y_t)$ can be expressed as

$$\mathbb{E}\left(X_t^{r_1}Y_t^{r_2}\right)=\sum_{(x,y)\in\mathbb{Z}^2}x^{r_1}y^{r_2}\mathbb{P}[(X_t,Y_t)=(x,y)]$$
$$=\int_{-\pi}^{\pi}\frac{da}{2\pi}\int_{-\pi}^{\pi}\frac{db}{2\pi}\langle\hat{\Psi}_t(a,b)|D_a^{r_1}D_b^{r_2}|\hat{\Psi}_t(a,b)\rangle$$
$$=(t)_{r_1+r_2}\int_{-\pi}^{\pi}\frac{da}{2\pi}\int_{-\pi}^{\pi}\frac{db}{2\pi}\sum_{j=1}^{3}\left(\frac{D_a\lambda_j(a,b)}{\lambda_j(a,b)}\right)^{r_1}\left(\frac{D_b\lambda_j(a,b)}{\lambda_j(a,b)}\right)^{r_2}|\langle v_j(a,b)|\hat{\Psi}_0(a,b)\rangle|^2+O(t^{r_1+r_2-1}), \tag{41}$$

with $D_a=i(\partial/\partial a)$, $D_b=i(\partial/\partial b)$, and $(t)_r=t(t-1)\times\cdots\times(t-r+1)$, where $\mathbb{E}(X)$ denotes the expected value of a random variable $X$. Obviously, we have $D_a\lambda_1(a,b)/\lambda_1(a,b)=D_b\lambda_1(a,b)/\lambda_1(a,b)=0$ because of the constant eigenvalue $\lambda_1(a,b)=1$. The eigenvalue $\lambda_1(a,b)$, hence, causes a Dirac $\delta$ function at the origin in the limit distribution which we are trying to prove. That means there is a possibility that localization occurs at the origin on the rescaled space $(X_t/t,Y_t/t)$. The measure of localization generally depends on the initial condition of the walker, which is characterized by the parameter $\alpha$, $\beta$, and $\gamma$ in this study. The dependence on the initial condition is expressed as the coefficient of the Dirac $\delta$ function. On the other hand, since we compute

$$\frac{D_a\lambda_j(a,b)}{\lambda_j(a,b)}=-(-1)^j\frac{(1+c)\sin\left(\frac{a+b}{2}\right)+(1-c)\sin\left(\frac{a-b}{2}\right)}{\sqrt{4-\left\{(1+c)\cos\left(\frac{a+b}{2}\right)+(1-c)\cos\left(\frac{a-b}{2}\right)\right\}^2}}\quad(j=2,3), \tag{42}$$

$$\frac{D_b\lambda_j(a,b)}{\lambda_j(a,b)}=-(-1)^j\frac{(1+c)\sin\left(\frac{a+b}{2}\right)-(1-c)\sin\left(\frac{a-b}{2}\right)}{\sqrt{4-\left\{(1+c)\cos\left(\frac{a+b}{2}\right)+(1-c)\cos\left(\frac{a-b}{2}\right)\right\}^2}}\quad(j=2,3), \tag{43}$$

the eigenvalues $\lambda_j(a,b)\,(j=2,3)$ give the continuous part in the limit density function. For the joint moments of the rescaled position $(X_t/t,Y_t/t)$, by putting $D_a\lambda_j(a,b)/\lambda_j(a,b)=x$ and $D_b\lambda_j(a,b)/\lambda_j(a,b)=y$ after $t\to\infty$, we get a convergence theorem

$$\lim_{t\to\infty}\mathbb{E}\left[\left(\frac{X_t}{t}\right)^{r_1}\left(\frac{Y_t}{t}\right)^{r_2}\right]=\int_{-\pi}^{\pi}\frac{da}{2\pi}\int_{-\pi}^{\pi}\frac{db}{2\pi}\sum_{j=1}^{3}\left(\frac{D_a\lambda_j(a,b)}{\lambda_j(a,b)}\right)^{r_1}\left(\frac{D_b\lambda_j(a,b)}{\lambda_j(a,b)}\right)^{r_2}|\langle v_j(a,b)|\hat{\Psi}_0(a,b)\rangle|^2$$
$$=\int_{-\infty}^{\infty}dx\int_{-\infty}^{\infty}dy\,x^{r_1}y^{r_2}\left\{\Delta(\theta;\alpha,\beta,\gamma)\delta_o(x,y)+\frac{\xi(x,y;\alpha,\beta,\gamma)}{2\pi^2(1-x^2)(1-y^2)}I_{\mathcal{D}}(x,y)\right\}, \tag{44}$$

with Eqs. (38)–(40). Equation (44) guarantees Theorem 2. ∎

In Fig. 5 we show the two examples of the continuous part in the limit density function for a representative initial state when the walker is evolved using the Grover coin.

## V. ENTANGLEMENT GENERATION IN THE THREE-STATE ALTERNATE WALK AND A FOUR-STATE WALK

From the earlier result of a four-state DTQW [10] and from the theorems presented in Secs. III and IV, we clearly see the presence of a Dirac $\delta$ function resulting in localization around the origin. These localized components are also accompanied by a diffusing component as a continuous part of the limit density function. In spite of the similarities, different dimensions of the coin space used for both the walks result in final states which are very different from one another. To make a fair comparison of the two kinds of localized walks, we can use the comparison of a spatial entanglement between the two-spatial dimension ($x$-$y$ spatial entanglement) which is common to both after tracing out the coin space from the final state [12,16].

In Fig. 6 we show the probability distribution for a configuration of the three-state alternate walk and the four-state walk

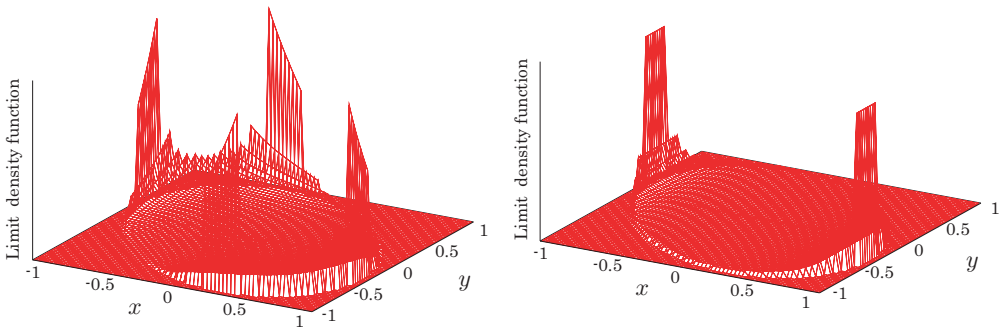


(a) $\alpha = \beta = \gamma = 1/\sqrt{3}$ (b) $\alpha = \gamma = 0$, $\beta = 1$

FIG. 5. (Color online) Continuous part of the limit density function ($c = -1/3$, $s = 2\sqrt{2}/3$).

resulting in localization. Though both probability distributions after 30 steps of the walk show localization manifesting from the evolution, the distributions are not identical to each other.

To make a comparison between these two walks, we calculate an entanglement measure called the negativity [24], defined by

$$N(\rho) = \frac{\|\rho^{T_b}\| - 1}{d - 1}, \tag{45}$$

where $\rho^{T_b}$ is the partial transpose of a state $\rho$ in $d_1 \otimes d_2$ ($d_1 \leqslant d_2$) quantum systems and $\|\cdot\|$ is the trace norm. This will bound the maximum value of the entanglement measure to 1 for the system of all dimensions.

In Fig. 7(a) we present the negativity between the coin and the position space, $N(\rho_{pp})$, where $\rho_{pp} = |\Psi_t\rangle\langle\Psi_t|$. We can see that for both the three-state and the four-state DTQW the value of negativity is nearly the same (close to unity) and only for the four-state walk do we see oscillations around the mean value. However, to compare the entanglement generated in different systems we need to consider the system of the same dimension. Therefore, as mentioned earlier in this section, by tracing out the coin space from the density operator $\rho_{pp}$ of both the three-state and the four-state DTQW we will be left with the reduced density operator $\rho_{xy}$ of the same dimension and that can be used to calculate the entanglement between the two spatial dimensions.

In Fig. 7(b) the negativity between the two spatial dimensions $[N(\rho_{xy})]$ is shown. We can see that the value of the negativity is very large for evolution using the three-state alternate walk compared to the four-state walk. This result is consistent with the results showing a higher spatial entanglement for a two-state alternate DTQW compared to the four-state walk [12,16]. This in general shows that the DTQW on a smaller Hilbert space results in a higher spatial entanglement in the system. Though it might not be of any immediate physical significance, it has the potential to be a resource when spatial entanglement is effectively tapped as a resource for quantum information protocols.

Before we conclude, we will look into the physical realizability of the three-state alternate walk on a two-dimensional lattice. A two-dimensional DTQW so far has been demonstrated using two walkers on a one-dimensional lattice [7]. This implementation was realized by exploiting the topologically equivalent of two walkers acting on a one-dimensional graph with one walker on a two-dimensional lattice. With the use of a single three-level system, one can avoid the use of coupled two-level system to implement walk on a two-dimensional lattice. Additional to that, in most of the three-level systems, decoupling one of the levels (state) from the remaining levels has been demonstrated. This allows the system to be reduced to the two-level system. Therefore, implementing DTQW in a three-level system can be engineered to reproduce both the wide spread probability distribution of the two-state alternate DTQW and localization of the four-state DTQW.

Physically realizable three-level systems are the particular physical realization of the qutrit state, namely, three-level atoms with energies $E_1$, $E_2$, and $E_3$. Atomic systems in the form of three-level systems have played a significant role in

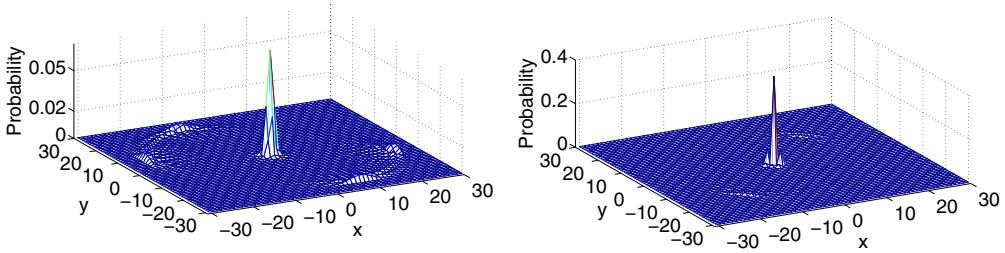


(a) Localization in the three-state alternate DTQW (b) Localization in a four-state DTQW

FIG. 6. (Color online) Probability distribution at time $t = 30$. (a) Three-state alternate walk with the parameters $\theta = \pi/2$, $\alpha = 0$, $\beta = 1$, and $\gamma = 0$, which give the coefficient $\Delta = (1 - 2/\pi)$. (b) Four-state walk with coin parameters $p = q = 1/2$ and initial state parameters $q_1 = 1/\sqrt{2}$, $q_2 = 1/\sqrt{2}$, $q_3 = 0$, and $q_4 = 0$ for the walk in Ref. [10], which give the coefficient $\Delta = (1 - 2/\pi)$.

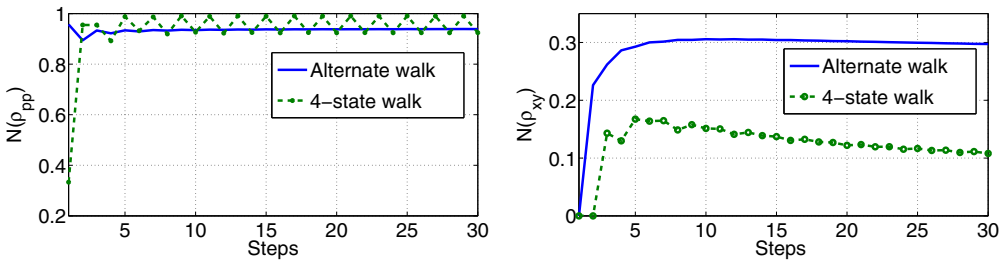


(a) Particle-position entanglement (b) Spatial entanglement ($X_t = Y_t$)

FIG. 7. (Color online) Negativity as a measure of entanglement for the three-state alternate walk and the four-state walk as a function of steps (time). (a) Negativity between particle and position space and (b) negativity between the two spatial dimensions ($x$-$y$).

demonstrating various interesting coherent phenomena and generate diverse quantum effects, for example, two-photon coherence [25], coherent multilevel photon ionization [26,27], and Stimulated Raman adiabatic passage (STIRAP) [28]. Recent experimental advancements have been able to demonstrate sufficient control over the three configurations of three-level systems (atoms) known as $\Lambda$, cascade, and $V$ configuration. In most of the three-level systems, decoupling of one of the level (state) from the remaining levels has been demonstrated. This allows the system to be reduced to the two-level system. Engineering the coupling between the energy levels and converting the energy difference between the energy levels to translational motion in position space, the coin and the shift operator can be designed in a three-level atomic system in optical lattice as it is done in two-level atoms [6].

A single photon as qutrit in Laguerre-Gaussian (LG) modes with states $|L\rangle$, $|G\rangle$, and $|R\rangle$ carrying orbital angular momenta of $-\hbar$, 0, and $\hbar$, respectively, is another physical system where the three-state alternate DTQW can be implemented.

## VI. DISCUSSION AND SUMMARY

We studied a three-state alternate DTQW starting from the origin and obtained two limit theorems. The walker, which has three coin states at each position, moves on a two-dimensional position space $\mathbb{Z}^2$ (square lattice) by alternately repeating a walk in the $x$ direction followed by a walk in the $y$ direction. The coin-flip operation for the evolution of the walk in each dimension was given by a parametrized unitary matrix which includes a Grover coin. One of the two limit theorems was the limit of a return probability defined by the probability that the walker returns to the starting point, and the other was a convergence in distribution for the position of the walker on a rescaled space by time. The return probability can be positive depending on both the initial condition at the origin and the coin-flip operator. The limit distribution in the convergence on the rescaled space has both a Dirac $\delta$ function at the origin and a continuous function with a compact support which is described by an ellipse. From these results, we see that the three-state alternate DTQW can localize around the origin. Using negativity as a measure of entanglement, we also showed that the entanglement generated between the two spatial dimensions using the three-state DTQW is higher than the spatial entanglement generated using the four-state DTQW.

Although we computed just the return probability at a long-time limit, we can also get the long-time limit of the probability $\mathbb{P}[(X_t, Y_t) = (x, y)]$ for any $x, y \in \mathbb{Z}$ according to Eqs. (32)–(34). It is, however, hard to calculate the limit due to the function $F(x, y)$ which is a single-variable integral in Eq. (27). To know the behavior of the walker after many steps at any position besides the origin, it would be an interesting future problem to compute the integral $F(x, y)$ and the limit $\lim_{t\to\infty} \mathbb{P}[(X_t, Y_t) = (x, y)]$.

## ACKNOWLEDGMENTS

T.M. acknowledges support from the Japan Society for the Promotion of Science. C.M.C. acknowledges support from the Department of Science and Technology, Government of India, through the Ramanujan Fellowship Grant No. SB/S2/RJN-192/2014.

[1] S. E. Venegas-Andraca, Quantum walks: A comprehensive review, Quant. Info. Proc. **11**, 1015 (2012).
[2] A. M. Childs, Universal Computation by Quantum Walk, Phys. Rev. Lett. **102**, 180501 (2009).
[3] N. B. Lovett, S. Cooper, M. Everitt, M. Trevers, and V. Kendon, Universal quantum computation using the discrete-time quantum walk, Phys. Rev. A **81**, 042330 (2010).
[4] M. Mohseni, P. Rebentrost, S. Lloyd, and A. Aspuru-Guzik, Environment-assisted quantum walks in photosynthetic energy transfer, J. Chem. Phys. **129**, 174106 (2008).
[5] J. K. Asbóth and H. Obuse, Bulk-boundary correspondence for chiral symmetric quantum walks, Phys. Rev. B **88**, 121406 (2013).
[6] M. Karski, L. Förster, J. Choi, A. Steffen, W. Alt, D. Meschede, and A. Widera, Quantum walk in position space with single optically trapped atoms, Science **325**, 174 (2009).
[7] A. Schreiber, A. Gábris, P. P. Rohde, K. Laiho, M. Stefanak, V. Potocek, C. Hamilton, I. Jex, and C. Silberhorn, A 2D quantum walk simulation of two-particle dynamics, Science **336**, 55 (2012).

[8] P. M. Preiss, R. Ma, M. E. Tai, A. Lukin, M. Rispoli, P. Zupancic, Y. Lahini, R. Islam, and M. Greiner, Strongly correlated quantum walks in optical lattices, Science **347**, 1229 (2015).

[9] T. D. Mackay, S. D. Bartlett, L. T. Stephenson, and B. C. Sanders, Quantum walks in higher dimensions, J. Phys. A **35**, 2745 (2002).

[10] K. Watabe, N. Kobayashi, M. Katori, and N. Konno, Limit distributions of two-dimensional quantum walks, Phys. Rev. A **77**, 062331 (2008).

[11] C. M. Chandrashekar, S. Banerjee, and R. Srikanth, Relationship between quantum walks and relativistic quantum mechanics, Phys. Rev. A **81**, 062340 (2010).

[12] C. Di Franco, M. McGettrick, and T. Busch, Mimicking the Probability Distribution of a Two-Dimensional Grover Walk with a Single-Qubit Coin, Phys. Rev. Lett. **106**, 080502 (2011).

[13] C. Di Franco, M. McGettrick, T. Machida, and T. Busch, Alternate two-dimensional quantum walk with a single-qubit coin, Phys. Rev. A **84**, 042337 (2011).

[14] C. Di Franco and M. Paternostro, Localizationlike effect in two-dimensional alternate quantum walks with periodic coin operations, Phys. Rev. A **91**, 012328 (2015).

[15] E. Roldán, C. Di Franco, F. Silva, and G. J. de Valcárcel, $n$-dimensional alternate coined quantum walks from a dispersion-relation perspective, Phys. Rev. A **87**, 022336 (2013).

[16] C. M. Chandrashekar and T. Busch, Decoherence in two-dimensional quantum walks using four-and two-state particles, J. Phys. A **46**, 105306 (2013).

[17] N. Inui, N. Konno, and E. Segawa, One-dimensional three-state quantum walk, Phys. Rev. E **72**, 056112 (2005).

[18] M. Štefaňák, I. Bezděková, and I. Jex, Continuous deformations of the Grover walk preserving localization, Eur. Phys. J. D **66**, 1 (2012).

[19] M. Štefaňák, I. Bezděková, I. Jex, and S. M. Barnett, Stability of point spectrum for three-state quantum walks on a line, Quantum Inf. Comput. **14**, 1213 (2014).

[20] M. Štefaňák, I. Bezděková, and I. Jex, Limit distribution of three-state quantum walks: The role of coin eigenstates, Phys. Rev. A **90**, 012342 (2014).

[21] T. Machida, Limit theorems of a 3-state quantum walk and its application for discrete uniform measures, Quantum Inf. Comput. **15**, 406 (2015).

[22] Y. Ide, N. Konno, T. Machida, and E. Segawa, Return probability of one-dimensional discrete-time quantum walks with final-time dependence, Quantum Inf. Comput. **11**, 761 (2011).

[23] G. Grimmett, S. Janson, and P. F. Scudo, Weak limits for quantum random walks, Phys. Rev. E **69**, 026119 (2004).

[24] S. Lee, D. P. Chi, S. D. Oh, and J. Kim, Convex-roof extended negativity as an entanglement measure for bipartite quantum systems, Phys. Rev. A **68**, 062304 (2003).

[25] D. Grischkowsky, M. M. T. Loy, and P. F. Liao, Adiabatic following model for two-photon transitions: Nonlinear mixing and pulse propagation, Phys. Rev. A **12**, 2514 (1975), and references therein.

[26] S. Adachi, H. Niki, Y. Izawa, S. Nakai, and C. Yamanaka, Experimental and numerical studies on population trapping in gd vapor, Opt. Commun. **81**, 364 (1991).

[27] E. Thiele, M. F. Goodman, and J. Stone, Concerning the effect of laser pulse shape on the product yield in collisionless mpd, Chem. Phys. Lett. **72**, 34 (1980).

[28] K. Bergmann, H. Theuer, and B. Shore, Coherent population transfer among quantum states of atoms and molecules, Rev. Mod. Phys. **70**, 1003 (1998).